Economic Geology, v. 120, no. 7, pp. 1735–1750

Regional Copper Isotope Variations in the Giant Mount Isa Copper Mineral System—Toward a Basinal Origin

David L. Huston,[1,†,*] Ryan Mathur,[2] Ioan Sanislav,[3] Jonathan Cloutier,[1] David Champion,[1,**] Vladimir Lisitsin,[4] Jo Whelan,[5] Adam C. Simon,[6] and Irene del Real[7]

[1]*Geoscience Australia, GPO Box 378, Canberra, Australian Capital Territory 2601, Australia*

[2]*Department of Geology, Juniata College, 1700 Moore St, Huntington, Pennsylvania 16652, USA*

[3]*Economic Geology Research Centre (EGRU), James Cook University, Townsville, Queensland 4811, Australia*

[4]*Geological Survey of Queensland, Level 4, 1 William St, Brisbane, Queensland 4000, Australia*

[5]*Northern Territory Geological Survey, GPO Box 4550, Darwin, Northern Territory 0801, Australia*

[6]*Department of Earth and Environmental Sciences, University of Michigan, Ann Arbor, Michigan 48109-1005, USA*

[7]*Department of Mining Engineering, Pontificia Universidad Católica de Chile, Santiago 7810000, Chile*

Abstract

Analysis of regionally altered mafic rocks for δ^{56}Fe and δ^{65}Cu in the Mount Isa mineral province has identified a 25- × 50-km ^{65}Cu-enriched zone to the east of the Mount Isa copper deposit. This δ^{65}Cu anomaly coincides with the northern part of a zone enriched in ^{56}Fe and depleted in copper. The timing of basalt alteration and the zones of ^{65}Cu enrichment and copper enrichment overlap, such that the high δ^{65}Cu zone is interpreted to mark the minimum extent of the mineral system that formed the Mount Isa copper deposit.

The observed ^{65}Cu enrichment in the altered mafic rocks can be modeled as residual copper left from copper depletion of the basalt, assuming that Rayleigh isotopic fractionation enriched the residual basalt in ^{65}Cu, closely matching the observed spatial distribution. Copper isotope, light stable isotope, and geochemical data from the ores and altered mafic rocks suggest that the ore fluid was an evolved brine sourced either from the Isa and/or Roper superbasins after the main contractional phase of the Isan orogeny, and not a metamorphic or magmatic-hydrothermal fluid.

Modeling of chalcopyrite deposition via Rayleigh fractionation using the δ^{65}Cu value of the modeled ore fluid results in an increase in δ^{65}Cu away from the point of ore fluid entry of about 0.8 to 1.0‰, consistent with an increase in δ^{65}Cu of ~1.0‰ away from major structures, as noted in a previous study. In addition to contributing to genetic understandings of mineral system processes, δ^{65}Cu data may enhance mineral exploration by identifying metal sources and deposit-scale zonation related to ore deposition.

Introduction

The Mount Isa province, in northwest Queensland, Australia, is one of the most intensely and complexly mineralized provinces in the world, containing world-class stratiform, shale-hosted zinc (e.g., Mount Isa zinc, Hilton-George Fisher, and Cannington), breccia-hosted copper (Mount Isa copper), and iron oxide copper-gold (IOCG: e.g., Ernest Henry) deposits. This province, and its extension to the northwest, is the largest global zinc province and a major copper-gold province.

Although still disputed by some (e.g., McGoldrick and Keays, 1990; Perkins, 1998; Cave et al., 2020), most workers in the region infer two broad mineralizing events in the Mount Isa province: (1) an earlier synbasin event that produced shale-hosted zinc deposits, and (2) a later syntectonic to post-tectonic event that formed breccia-hosted copper and IOCG deposits (Large et al., 2005; Williams et al., 2005). In this case, the term "synbasin," used herein, refers to geologic processes associated with basin formation and includes processes with timings that range from synsedimentation, through diagenesis and early epigenesis. The terms "syntectonic" and "post-tectonic" refer to processes after the basin has largely lithified and been subject to deformational events. In detail, however, these two broad events are complex. The early event involved several pulses of zinc mineralization, mostly between 1675 and 1575 Ma (Large et al., 2005; Huston et al., 2006); the later event involved pulses of copper-cobalt, copper-gold-cobalt, and uranium mineralization, mostly between 1540 and 1500 Ma (Perkins et al., 1999; Gregory et al., 2005; Duncan et al., 2011). Untangling the drivers and fluid and metal sources for the two events has been difficult and has led to much disagreement (Heinrich et al., 1989, 1995; McGoldrick and Keays, 1990; Perkins, 1998; Sanislav et al., 2023).

To determine the drivers and sources, studies over the last 50 years have used techniques ranging from lithological, alteration, and structural mapping, through whole-rock geochemical analyses, to stable and radiogenic isotopic analyses at both deposit and regional scales (Heinrich et al., 1989, 1995; McGoldrick and Keays, 1990; Hannan et al., 1993; Perkins, 1998; Gregory, 2006; Champion et al., 2020a, b; Huston et al., 2023; Sanislav et al., 2023). Although there is general consensus that the copper in the Mount Isa copper orebodies was

[†]Corresponding author: email, David.Huston@anu.edu.au

[*]Present address: Research School of Earth Sciences, Australian National University, Acton, Australian Capital Territory 2601, Australia.

[**]Retired

ISSN 0361-0128; doi:10.5382/econgeo.5177; 16 p.
Digital appendices are available in the online Supplements section.

Submitted: August 25, 2024/Accepted: June 20, 2025

leached from basaltic sources (Heinrich et al., 1995; Gregory, 2006; Champion et al., 2020a, b; Sanislav et al., 2023), three different interpretations of fluid source have been advocated: (1) basinal brines, (2) metamorphic fluids, and (3) magmatic-hydrothermal fluids (Heinrich et al., 1989, 1995; Sanislav et al., 2023).

In recent years, analytical advancements have enabled the analysis of metallic (e.g., copper, iron, and zinc) stable isotopes, a tool now commonly used at the deposit scale (e.g., Mathur and Zhao, 2023), including for the Mount Isa copper deposit (Sanislav et al., 2023), but not used previously at the regional scale. Here, we present a regional study of copper and of iron isotopes on mafic rocks (including basalt and dolerite), which are interpreted by many (e.g., Heinrich et al., 1995; Cooke et al., 1998; Gregory, 2006; Champion et al., 2020a, b; Sanislav et al., 2023) as metal sources for either the early and/or the later mineralizing events in the Mount Isa province.

This study differs from the deposit-scale copper isotope study of the Mount Isa copper deposit presented by Sanislav et al. (2023). Whereas that study analyzed ore minerals (chalcopyrite) from mineralized and altered host rocks, the present study presents whole-rock analyses from samples collected at the mineral province scale. Whereas the former study established ore-related depositional processes, the present study targets processes associated with metal leaching. As far as we are aware, this is the first regional study using metallic isotopes to assess metal source. Our data yield new insights into mineralizing processes and may provide exploration vectors. In this contribution, we concentrate on implications for the Mount Isa copper mineral system, with future contributions targeting the shale-hosted zinc and IOCG systems of the region.

Geology and Metallogenesis of the Mount Isa Mineral Province

The Mount Isa province (Fig. 1A), which forms the southeastern part of the Greater McArthur basin, or North Australian basin system, consists of three Paleo-Mesoproterozoic superbasins (Southgate et al., 2013; Gibson et al., 2016; Gibson and Edwards, 2020). The 1790 to 1740 Ma Leichhardt superbasin, which formed during initial rifting of the North Australian craton, consists mostly of lacustrine to fluviatile siliciclastic rocks and tholeiitic basalt (Jackson et al., 2000; Withnall and Hutton, 2013). The basaltic rocks range up to 8 km in thickness (Gibson et al., 2018).

The overlying 1730 to 1640 Ma Calvert superbasin comprises shallow to deep marine carbonate and siliciclastic rocks with local mafic sills and lavas (Jackson et al., 2000; Southgate et al., 2000; Withnall and Hutton, 2013; Gibson et al., 2016). The Calvert superbasin was terminated by the contractional ca. 1640 Ma Riversleigh tectonic event (D_1), which is expressed stratigraphically as an unconformity or disconformity (Gibson et al., 2016). The overlying 1640 to 1590 Ma Isa superbasin consists of passive margin siliciclastic and carbonate rocks without coeval volcanic rocks (Southgate et al., 2000). The Isa superbasin was terminated by the early (1600–1580 Ma: Giles et al., 2006; Li et al., 2020) contractional phase of the Isan orogeny (D_2).

To the north and west of the Mount Isa province, rocks of the Greater McArthur basin are overlain unconformably by strata of the Roper-South Nicholson basin. As the Roper basin, which lies north of the Murphy inlier, is generally correlated with the South Nicholson basin to the south of the inlier, we refer to the combined entity here as the Roper-South Nicholson basin. The age of this basin, which is dominated by fluviatile to shallow marine sandstone with lesser siltstone and mudstone, is poorly constrained between the ca. 1589 ± 3 Ma age of the unconformably underlying Balbarini dolostone (Page et al., 2000) and the ca. 1327.5 ± 0.6 Ma age of the Derim Derim dolerite (Abbott et al., 2001; Bodorkos et al., 2021). The only stratigraphic ages for the Roper-South Nicholson basin are provided by tuff and volcaniclastic units, dated at 1492 ± 4 Ma (Jackson et al., 1999) and ca. 1483 Ma (Anderson et al., 2019), stratigraphically located within the lower central part of the succession.

The basins of the Mount Isa province have been affected by several tectonic events: the ca. 1640 Ma Riversleigh event (Gibson and Edwards, 2020) and several events collectively grouped as the Isan orogeny at ca. 1600 to 1500 Ma (Betts et al., 2006; Giles et al., 2006; Li et al., 2020). The Isan orogeny includes an early phase (1600–1580 Ma), characterized by NW-SE– and then E-W–directed contraction and metamorphism, followed by a later phase (1550–1500 Ma), the character of which is disputed. Some authors (e.g., Lister et al., 1999; Giles et al., 2006; Abu Sharib and Sanislav, 2013) have inferred contraction or transpression, whereas Li et al. (2020) inferred E-W–directed extension for the latter phase.

These basinal strata have been intruded by granitic rocks (commonly with coeval volcanic rocks) at ca. 1740 to 1710 Ma, ca. 1690 to 1650 Ma, and ca. 1550 to 1500 Ma (Withnall and Hutton, 2013). The 1550 to 1500 Ma event produced the Williams-Naraku Suite of trondhjemite, followed by largely A-type granites (Withnall and Hutton, 2013), which accompanied the extensional phase of the Isan orogeny according to Li et al. (2020).

As mentioned above, two broad metallogenic events affected the Mount Isa province: the 1675 to 1575 Ma stratiform zinc-lead-silver event and the 1540 to 1500 Ma discordant copper and copper-gold event. The epigenetic Mount Isa copper deposit has an age of 1523 ± 6 Ma (Perkins et al., 1999), which overlaps with the ages of IOCG deposits to the east (1540–1500 Ma: Duncan et al., 2011; Williams, 2022) and the ages of chlorite-altered basalt (1534 ± 8 Ma; Perkins et al., 1999), and albitite-hosted uranium deposits (e.g., Valhalla at 1543 ± 15 Ma; Polito et al., 2009) to the north of Mount Isa. This age also overlaps with the age of the Williams-Naraku magmatic event and, possibly, the age of the earliest strata of the Roper-South Nicholson basin.

Regional-scale alteration studies (Table 1) indicate that rocks of the Mount Isa province have been extensively altered, perhaps best developed in basaltic rocks (Hannan et al., 1993; Heinrich et al., 1995; Cooke et al., 1998; Gregory, 2006; Champion et al., 2020a, b). Wyborn (1987), Hannan et al. (1993), and Heinrich et al. (1995) documented several styles of regional alteration assemblages that affected 1790 to 1760 Ma basaltic rocks of the Leichhardt superbasin in the vicinity of the Mount Isa copper deposit: syndeformational epidote + sphene, fault/shear-hosted chlorite ± albite, and fracture-related carbonate + hematite. The chlorite (± albite ± rutile) assemblage is developed extensively below the Mount Isa copper deposit (Hannan et al., 1993). Cooke et al. (1998) and

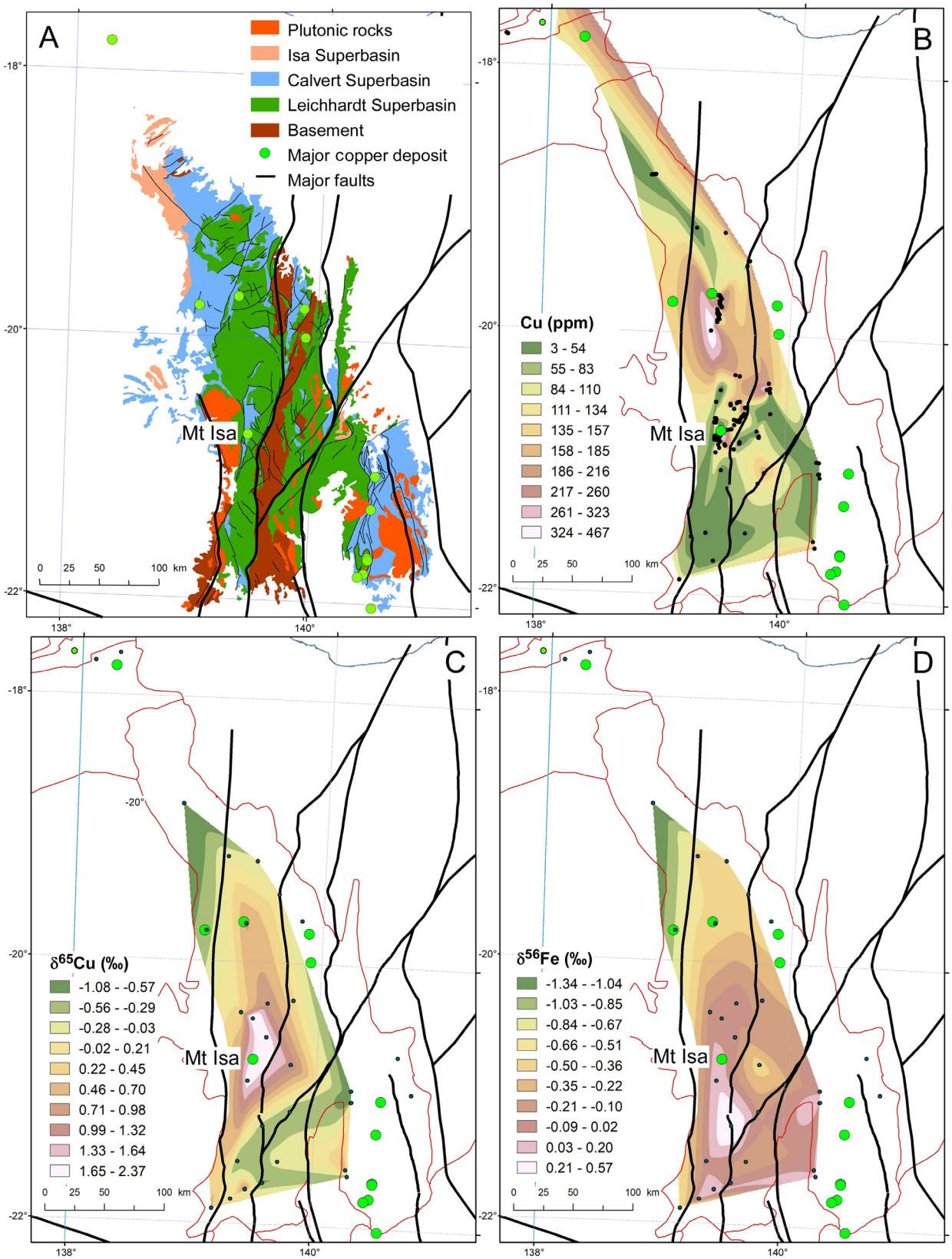

Fig. 1. Maps showing (A) geology of the Mount Isa province, (B) spatial variations in copper concentrations in 1790 to 1760 Ma basaltic rocks, (C) spatial variations in $\delta^{65}Cu$ from 1790 to 1760 Ma basaltic rocks, and (D) spatial variations in $\delta^{56}Fe$ from 1790 to 1770 Ma basaltic rocks. Part (A) is modified from Gibson and Edwards (2020).

Table 1. Characteristics of Regional Alteration Assemblages that Affect Mafic Rocks, Mount Isa Province

Alteration assemblage	Mineralogical characteristics	Geochemical characteristics (selected elements)	Relative timing and age	Comments	Sources
K-feldspar ± chlorite					
	Chlorite-K-feldspar Chlorite-orthoclase-quartz ± dolomite ± sericite ± actinolite ± albite ± anatase K-feldspar Orthoclase-quartz ± sericite ± hematite ± dolomite ± anatase ± barite	Chlorite-K-feldspar Gains—Mg, LOI Losses—total Fe, Ca, Sr, Pb, Zn Immobile—Si K-feldspar Gains—K, U Losses— total Fe, Mg, Ca, Na, LOI, Cu, Zn, Pb	Interpreted to be syn-Calvert; associated with shale-hosted Zn-Pb mineralizing events at 1665–1575 Ma	Appears to mainly or only affect 1730–1660 Ma mafic units Alteration involves two stages: unaltered basalt → chlorite and feldspar → feldspar	Cooke et al. (1998); Champion et al. (2020a, b)
Epidote-sphene					
	Epidote-quartz-sphene ± actinolite ± chalcopyrite ± pyrite ± hematite	Gains—Si, Fe^{3+}, Ca, S, Sr, Co, U, Pb Losses—Fe^{2+}, Mg, H_2O, Na, K, Cu, Zn Immobile—total Fe, CO_2	Hannan et al. (1993) interpreted assemblage to have formed during low-grade burial metamorphism and greenschist facies regional metamorphism Heinrich et al. (1995) indicated some epidote assemblages crosscut metamorphic textures	Occurs mostly in flow-top breccias from 1790 to 1760 Ma mafic units	Hannan et al. (1993); Heinrich et al. (1995)
Calcite-albite- magnetite					
	Calcite-albite-magnetite-hematite- quartz ± chlorite ± biotite (trace chalcopyrite, pyrite and bornite)	Gains—Si, Fe^{3+}, Ca, Na, CO_2, S, Cu, U Losses—Fe^{2+}, Mg, K, H_2O, Sr, Ni, Zn Immobile—total Fe, Pb	Described as possibly cross-cutting D_2 (Isan) faults Dated at ca. 1834 Ma by Perkins et al. (1999)	Centered on km-scale fracture zones	Heinrich et al. (1995); Perkins et al. (1999)
Chlorite (± albite ± rutile)					
	Chlorite-quartz-albite-rutile ± sericite (with local quartz ± dolomite ± calcite ± pyrite ± chalcopyrite veinlets)	Gains—Fe^{2+}, Mg, H_2O, S Losses—Fe^{3+}, Ca, Na, K, CO_2, Sr, Cu Immobile—Si, total Fe	Heinrich et al. (1995) indicate that the chlorite-rutile assemblage was coeval with or slightly postdated the calcite-albite-magnetite assemblage, indicating age of ca. 1534 Ma		Hannan et al. (1993); Heinrich et al. (1995); Perkins et al. (1999)

Abbreviation: LOI = loss on ignition

Champion et al. (2020a, b) documented extensive K-feldspar- and chlorite-dominant assemblages in younger (1730–1660 Ma) basaltic rocks, particularly in the extension of the Mount Isa province to the north. Geochemical studies by Heinrich et al. (1995), Cooke et al. (1998), and Champion et al. (2020a, b) suggested that the K-feldspar-dominant and chlorite ± albite assemblages have lost significant copper, both in the older and younger basaltic units. These altered basalts were targeted for metallic isotopic analysis in this study.

Analytical Methods and Data Compilation

This study emanates from a regional-scale geochemical investigation of the Greater McArthur basin that documented geochemical variations of a range of rock types within this basin system (Champion et al., 2020a, b). The Geoscience Australia geochemical database was queried for existing analyses, both from Geoscience Australia (and its predecessors) and external, published sources (e.g., Cooke et al., 1998). During this compilation, undersampled regions were identified, and a systematic sampling program from core libraries of the Geological Survey of Queensland and Northern Territory Geological Survey was undertaken. These samples were analyzed for major elements and a range of trace elements, and the new data and existing data were combined to enable mapping of spatial variations in geochemistry of the basin system. The complete geochemical data set is available in Champion et al. (2020c), and results are discussed by Champion et al. (2020a, b).

A subset of this sample set, consisting of 44 samples, with an additional four replicate analyses, was selected for spatial coverage as well as variations in alteration assemblages and whole-rock geochemistry. This subset was analyzed for copper and iron isotope compositions at Juniata College. For each sample, approximately 50 mg of rock powder was dissolved in 2 mL of ultrapure 18 M HF acid and dried. The remaining salts were dissolved in 4 mL of ultrapure aqua regia. Complete dissolution was visually confirmed. The aqua regia was dried, and these salts were used for ion exchange column chromatography using BioRad MP-1 anion exchange resin (Cl form, 100–200 grain size). The protocol was repeated twice on each rock sample. Details of the method are presented by Mathur et al. (2009, 2012). Yields for both Fe and Cu were above 92%, as determined volumetrically. Given that analytical uncertainties for copper and iron geochemical analyses are typically 5 to 10% depending on method, such yields are consistent with the total extraction of both copper and iron during isotopic analysis. The samples were measured on the Neptune Plus multicollector-inductively coupled plasma-mass spectrometer (MC-ICP-MS) at Juniata College using methods of Mathur et al. (2012) and Kempton et al. (2022). Mass bias was corrected by standard bracketing. The isotope values are reported for Cu relative to NIST976 and Fe relative to IRMM-14 in traditional per mil units. All Fe isotope data were monitored and confirmed for mass dependence using $\delta^{57}Fe$. QA/QC of the measurements was monitored through analysis of US Geo-

logical Survey (USGS) rock standards (BVHO-2 and AVG-2) and solution standards (internal 1838 USA cent for Cu and SRM 3126a for Fe). All values measured for both elements fall within error of reported values in Liu et al. (2015), Sossi et al. (2015), and Mathur et al. (2009). Each standard was measured more than 5 times; 2σ uncertainties are 0.1 and 0.09‰ for δ^{65}Cu and δ^{56}F, respectively.

The data were contoured spatially using natural neighbor interpolation and natural breaks in data values. This method produces results akin to those using manual contouring (Champion and Huston, 2023). As this contouring method does not consider vertical zonation, an average value was used for multiple data obtained from drill core samples.

Complete location information, isotopic analyses, and whole-rock analyses for all samples of Mount Isa regional basalt analyzed in this study are presented in Appendix 1. Ore and chalcopyrite δ^{65}Cu analyses from IOCG deposits in the Cloncurry district and the Candelaria district in Chile are presented in Appendix 2.

Results

In order to document geochemical variations caused by regional alteration of mafic rocks in the Greater McArthur basin, Figure 2 shows variations in copper and sulfur superimposed on MgO-Al_2O_3-K_2O (by weight) ternary diagrams for all mafic rock data from the compilation of Champion et al. (2020c: Fig. 2A, D), the 1790 to 1760 Ma subset (Fig. 2B and 2E), and the 1730 to 1660 Ma subset (Fig. 2C, 2F). The geochemical data for all samples indicate four geochemical trends from the generic basaltic composition of Cox et al. (1979). This composition was used because analyses of unequivocal unaltered basalt from the Greater McArthur basin are not available.

The first trend extends from the unaltered basalt composition toward clinochlore (dark-green line in Fig. 2A, D) and is interpreted to be related to the ca. 1530 Ma chlorite ± albite regional alteration event. As the clinochlore end member is approached, this trend is marked by decreases in concentrations of both copper (mostly <23 ppm: Fig. 2A) and sulfur (mostly <200 ppm: Fig. 2D). The low sulfur, and particularly low concentrations of copper in these trends, indicate that, when present, sulfide minerals, including chalcopyrite, are very uncommon in these altered rocks.

The second trend (dark-brown arrow) extends from unaltered basalt toward epidote and is interpreted to be related to the epidote + sphene alteration assemblage. Unlike the other alteration trends, this trend is characterized by generally high, though erratic, concentrations of copper and sulfur (mostly >59 ppm and >200 ppm, respectively) as epidote is approached. Trace to minor amounts of copper-iron sulfide minerals accompanied this alteration assemblage (Table 1).

The third trend (dark-blue arrow) extends from unaltered basalt toward the phengite-muscovite join and is interpreted to reflect a sericitic alteration assemblage not recognized in previous studies. Near the phengite-muscovite end member, this trend is characterized by very low copper (mostly <7 ppm) and sulfur (mostly <70 ppm) concentrations, making it unlikely that copper-iron sulfide minerals were present in this assemblage. This trend contains the fewest analyses and,

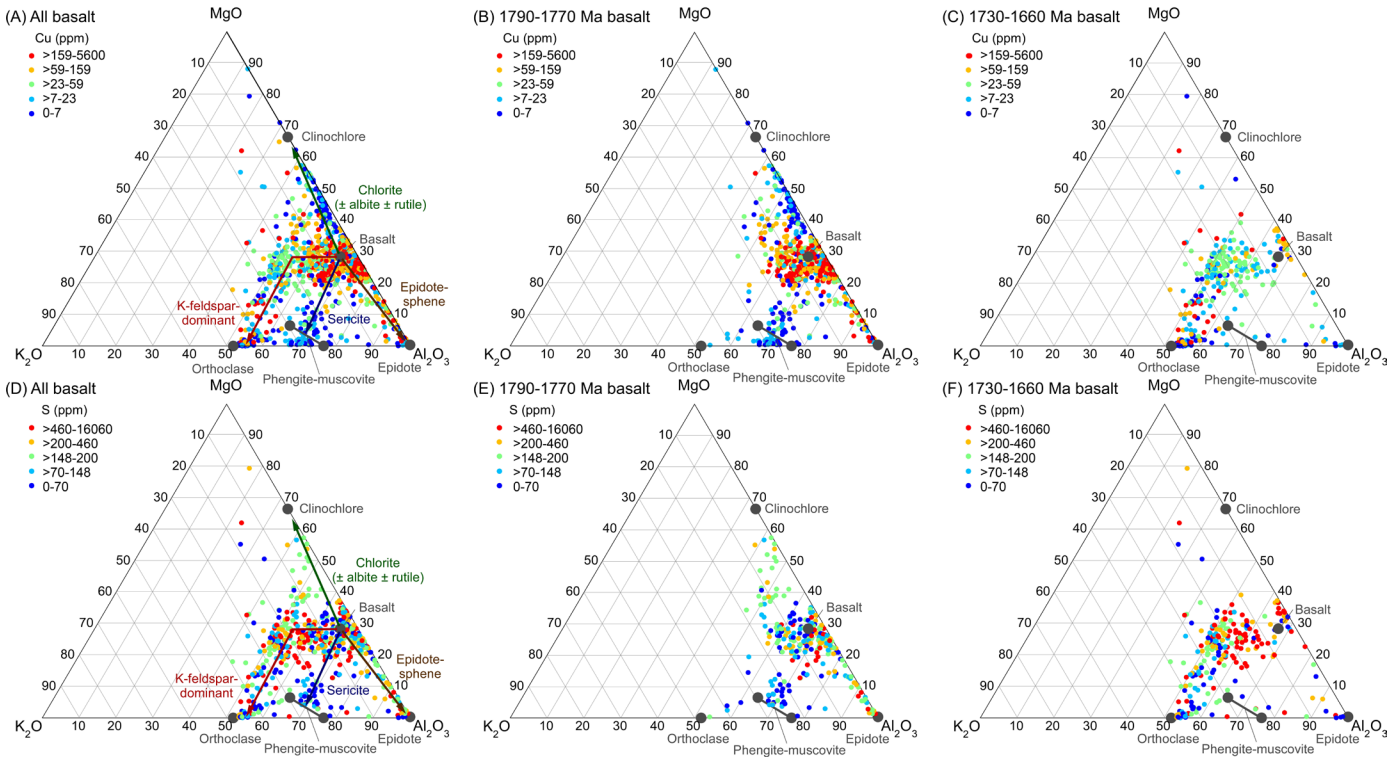

Fig. 2. Concentrations of copper (A-C) and sulfur (D-F) superimposed on MgO-Al_2O_3-K_2O ternary diagrams for all mafic rocks (A, D), 1790 to 1760 Ma mafic rocks (B, E), and 1730 to 1660 Ma mafic rocks (C, F) using data from Champion et al. (2020c). Symbol color indicates copper and sulfur concentrations for individual analyses (dark blue for lowest grading to red for highest).

when plotted on a map, is the most spatially restricted, being present only in the Leichhardt River domain in the western Mount Isa province (equivalent to the "Leichhardt River Fault Trough" of Derrick, 1982) near the eastern contact with basement rocks (Kalkadoon-Leichhardt domain).

The fourth trend (kinked red arrow) extends from unaltered basalt, initially by an increase in K_2O/Al_2O_3, and then toward an orthoclase end member. This trend likely relates to inferred 1675 to 1575 Ma K-feldspar ± chlorite alteration associated with the shale-hosted zinc-lead-silver deposits (Cooke et al., 1998; Champion et al., 2020a, b). Near the orthoclase end member, this trend is characterized by low copper (mostly <23 ppm) and sulfur (mostly <200 ppm), although some samples have higher concentrations. As a consequence, Cu-Fe sulfide minerals are likely to be uncommon in most samples within this alteration assemblage. When all mafic analyses are considered, copper concentrations broadly correlate with sulfur concentrations (Fig. 3A; $r = 0.238$, $n = 551$, $p = 1 \times 10^{-8}$), confirming observations from Figure 2.

In addition to the spatial restriction on the sericitic assemblage, the alteration assemblages also appear to be restricted to mafic rocks of different ages. The patterns in Figure 2B, C and 2E, F indicate that the chlorite ± albite, epidote ± sphene, and sericitic alteration assemblages are almost entirely restricted to the 1790 to 1760 Ma mafic rocks, whereas the K-feldspar ± chlorite assemblage is almost entirely restricted to the 1730 to 1660 Ma mafic rocks.

With the exception of the lack of a sericitic trend, trends observed in samples selected here for copper and iron isotope analysis are similar to those observed for the full Champion et al. (2020c) data set, including differences in the style of alteration affecting the 1790 to 1760 Ma and 1730 to 1660 Ma mafic rocks and the copper concentration trends (Fig. 4A, B). The lack of a sericitic trend can be ascribed to the apparently restricted geographical extent of samples that define this trend, and the relatively small number of samples analyzed for isotopes.

The highest δ^{65}Cu values occur in Cu-poor samples. Eleven of 14 samples with δ^{65}Cu above 1.0‰ have copper concentrations below 70 ppm, with most below 50 ppm (Fig. 3B). Lower δ^{65}Cu values (<1.0‰) occur in samples with a wide range of copper concentrations, up to 300 ppm.

As alteration can cause major changes in total mass of a rock, using the absolute concentrations of metals can be misleading. To alleviate this issue, Halley et al. (2016) and Halley (2020) preferred the use of Cu/Sc ratios to identify copper mobility relative to scandium, the latter serving as an immobile element. These studies reported background Cu/Sc ratios of 2.0 to 2.5, with ratios below this threshold indicating copper depletion. Like copper concentrations, δ^{65}Cu values above 1.0‰ are also associated with Cu/Sc ratios below 2.5 (10 of 11 samples), for both the younger and older age groups of basalt samples. Hence, as also seen in the ternary diagrams, high δ^{65}Cu is almost uniformly associated with regional copper depletion. However, lower δ^{65}Cu values (<1.0‰) can be associated with both copper enrichment (to 300 ppm Cu and to 12 Cu/Sc) and depletion (Fig. 3B, C).

If ~100 ppm is conservatively taken as the most likely concentration of copper in unaltered mafic rocks in the Mount Isa province, a large proportion of samples have lost a significant (i.e., more than 50%) portion of their copper (Figs. 2A-C, 3A-C, 4A, B). When weighted by the number of analyses across all areas, data from Gregory (2006) indicate that the Cromwell and Pickwick metabasalts have average copper concentrations of 163 and 111 ppm, respectively. As these rocks have been extensively altered, and copper has been removed and added during this alteration (e.g., Heinrich et al., 1995; Gregory, 2006), these estimates must be considered approximations. For comparison, fresh, recently erupted tholeiitic basalt from Hawaii has an average copper concentration of 98 ppm (West et al., 1992). Similarly, a large proportion of samples have Cu/Sc ratios below 2.5, which also indicates copper loss.

Figure 3D plots variations between δ^{65}Cu and δ^{56}Fe for both age groups. No statistically significant correlation was identified between these two parameters for the full data set. The range in δ^{56}Fe (–0.51 to 0.58‰; excluding one outlier at –1.35‰) is much narrower than the range in δ^{65}Cu (–1.09–2.66‰; excluding two outliers at –2.21 and 3.52‰).

Spatially, copper contouring defines two zones of copper depletion (Cu <83 ppm) in the southern part of the Mount Isa province and one, less well-defined zone in the northern part of the province (Fig. 1B). The first zone consists of a strip along the eastern margin of the contoured area. IOCG deposits of the Cloncurry district are located further east of this zone in a region that lacks data. The second zone occurs in the southwesternmost part of the province and has two fingers that extend northward, with the western finger passing just to the west of the Mount Isa copper deposit. This zone of copper depletion was also documented by Gregory (2006) in the immediate vicinity of Mount Isa. The deposit itself is located within a small copper-enriched zone just to the east of this finger that may be the result of low-grade mineralization adjacent to the orebody. Basalt in the central part of the province is also enriched in copper, relative to elsewhere in the province, with a narrow copper-depleted zone present in the northwest part of the province.

The highest δ^{56}Fe values (> –0.2‰) broadly coincide in space with the two southern copper-depleted zones. The western ^{56}Fe-enriched zone broadly defines a N-S–trending feature that extends to the Mount Isa copper deposit from the south (Fig. 1D). To the north, δ^{56}Fe decreases to values of less than –1‰. The highest δ^{65}Cu values (>0.98‰) define a spatially well-constrained triangular zone. The Mount Isa copper deposit occurs along the western margin of this N-S–trending zone, which has dimensions of 25 km × 50 km (Fig. 1C). δ^{65}Cu values decrease to the north and south of this zone, with the lowest values of less than –1‰ occurring in the north. Overall, the Mount Isa copper deposit is spatially associated with a ^{65}Cu-enriched zone that overlaps the northern part of a zone of copper depletion and ^{56}Fe enrichment.

Discussion

Determining the fluid and metal sources of the Mount Isa copper deposit is essential to understanding its origin, which, other than the Olympic Dam deposit in South Australia, has the largest copper endowment of any single Australian copper deposit. This information is vital, not only from a process point of view, but also in developing exploration models for this deposit type, both within Australia and overseas. Table 2 summarizes the fluid characteristics for both the Mount

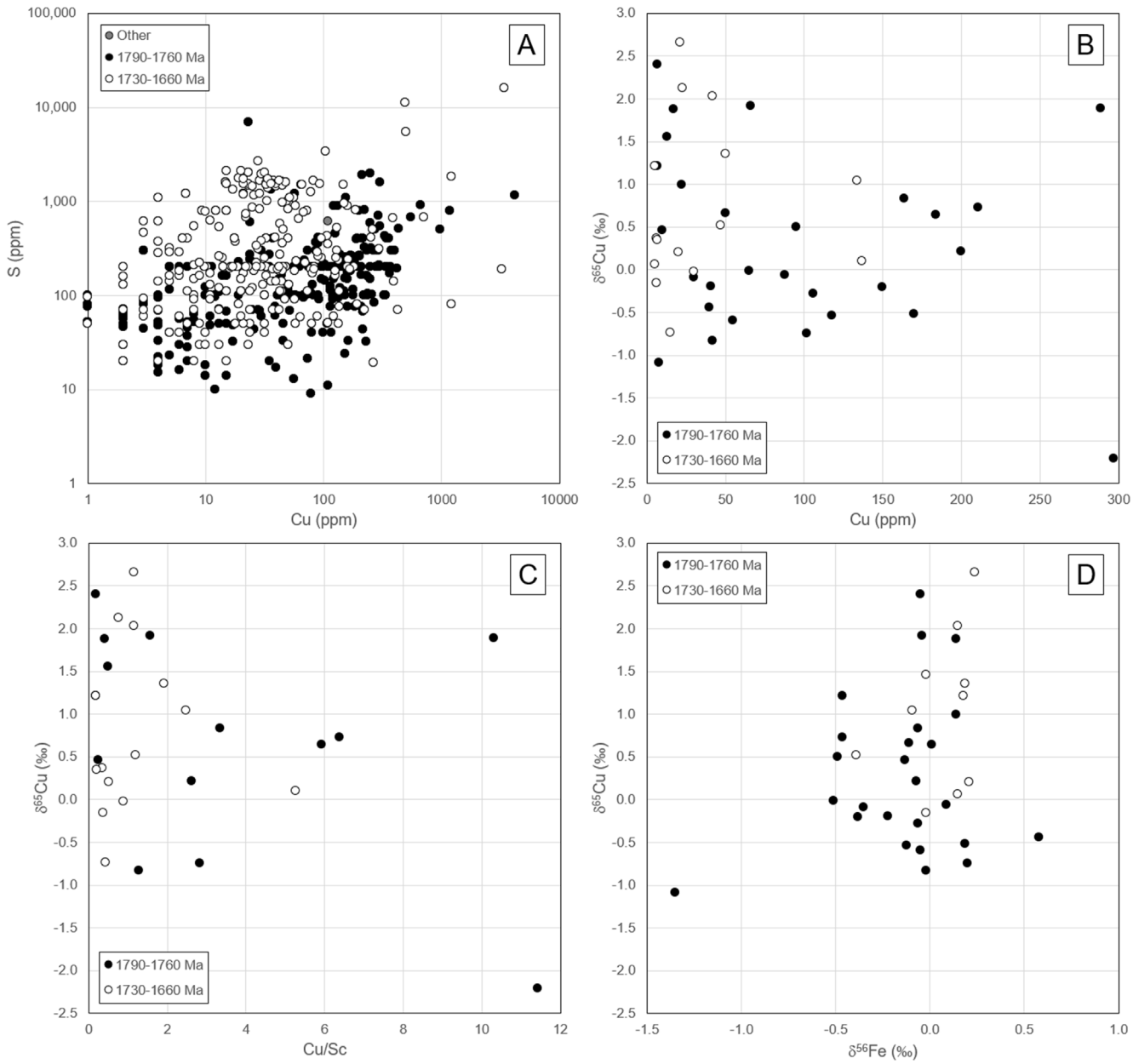

Fig. 3. Scattergrams from the Mount Isa province showing (A) relationship between copper and sulfur for all mafic rocks, (B) relationship between copper and δ^{65}Cu for all basaltic rocks, (C) relationship between Cu/Sc and δ^{65}Cu, and (D) relationship between δ^{65}Cu and δ^{56}Fe. Data for (A) include all analyses from Champion et al. (2020c); data for (B) to (D) include only samples for which isotopic data are available; data for (C) include only data for which scandium analyses exist. One sample with δ^{65}Cu = 1.46‰, Cu = 1220 ppm, and Cu/Sc = 45 is not shown in (B) and (C).

Isa copper mineralizing fluid and the basalt-altering fluid (Heinrich et al., 1989, 1993, 1995; Waring, 1990). Assuming that the deposit is epigenetic and formed during or after regional deformation and metamorphism (i.e., ca. 1525 Ma: Perkins et al., 1999), different possibilities for fluid and metal sources are presented in Table 3 and discussed below.

Regional alteration: Timing, overprinting, and copper depletion

Previous studies and our geochemical data indicate that mafic rocks in the Greater McArthur basin have been altered to four different assemblages defined by trends toward the composition of minerals that define the assemblage on the MgO-Al_2O_3-K_2O ternary diagram: (1) chlorite ± albite, (2) epidote + sphene, (3) sericite (phengite-muscovite), and (4) K-feldspar ± chlorite. Based on geochemical and inferred mineralogical characteristics, these assemblages can be correlated with alteration assemblages documented by previous workers (Hannan et al., 1993; Cooke et al., 1998; Champion et al., 2020a, b). We interpret the chlorite ± albite and epidote + sphene assemblages to correspond to the chloritic assemblage and epidosite of Hannan et al. (1993). Despite uncertainties

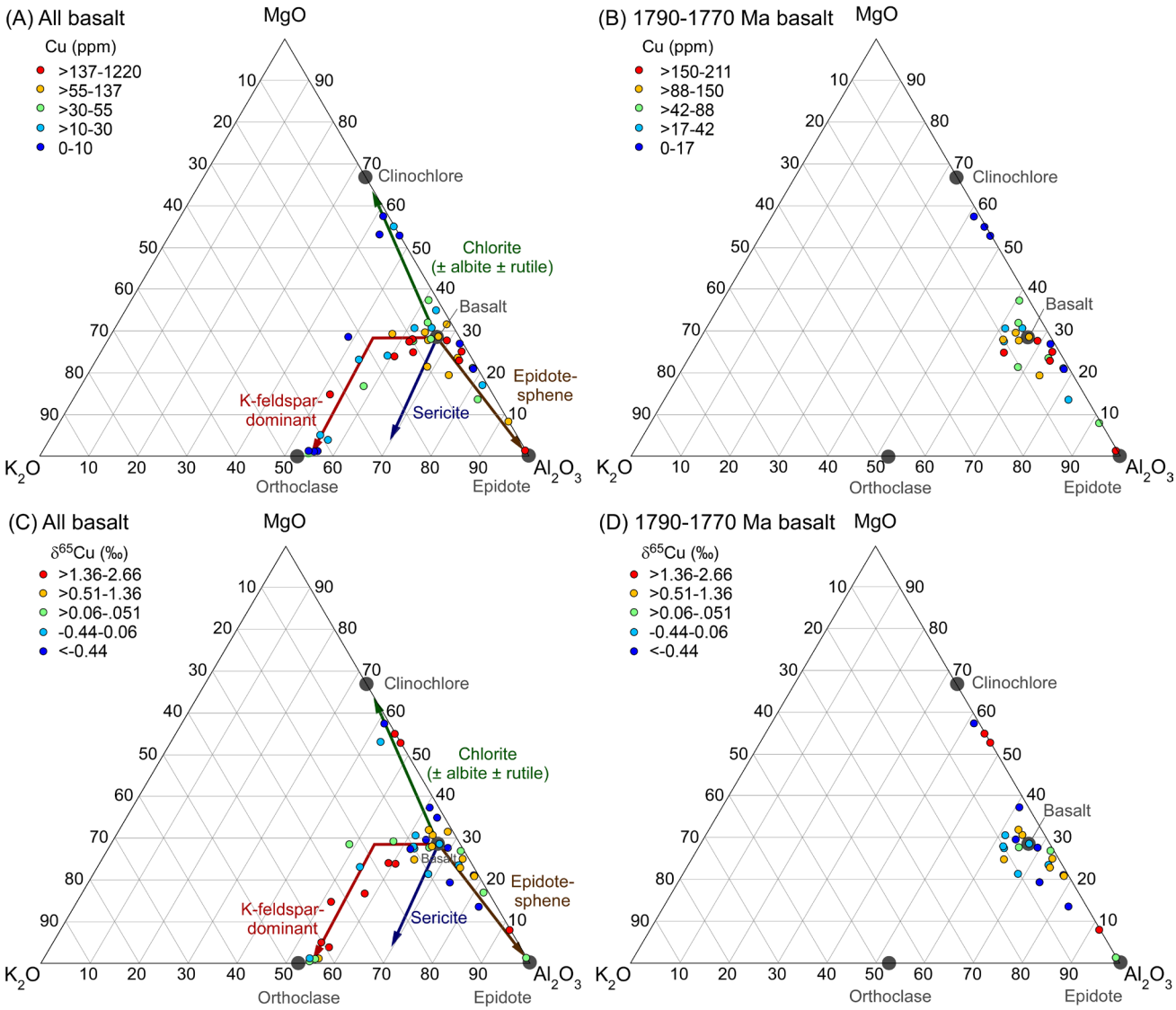

Fig. 4. Copper concentrations (A, B) and δ^{65}Cu analyses (C, D) superimposed on MgO-Al_2O_3-K_2O ternary diagrams for all mafic rocks (A, C), and 1790 to 1760 Ma mafic rocks (B, D). Symbol color indicates copper and sulfur concentrations for individual analyses (dark blue for lowest grading to red for highest). Data include only those samples for which isotopic data (this study) are available.

Table 2. Characteristics of Fluids of the Mount Isa Copper Mineral System (data from Heinrich et al., 1989, 1993, 1995; Kendrick et al., 2006)

	Ore fluid, Mount Isa copper deposit	Altering fluid, chlorite (± albite ± rutile) alteration assemblage
Temperature	T_h = 130°–280°C (mostly 140°–180°C); T_m = 300°–325°C[1]	T_h = 200°– 250°C; T_m = 300°–325°C[1]
Salinity	10–20 wt % NaCl evquiv	8–15 wt % NaCl equiv
Gases	X_{CO_2} < 0.02; X_{CH_4} ~ 0.00–0.02	Possible CH_4
Pressure	P_{fluid} = 1.1–1.8 kbar; depth = 6.1–6.6 km	
Light stable isotopes	$\delta^{18}O_{quartz}$ = 11.5–13.0‰ (n = 8); $\delta^{18}O_{fluid}$ = 3.6–5.1‰[2]; δD_{fluid} = –72 to –35‰ (from fluid inclusion measurements)	$\delta^{18}O_{quartz}$ = 8.6–10.7‰ (three of four analyses between 10.4 and 10.7‰; measured off figure 11 of Heinrich et al., 1995); $\delta^{18}O_{fluid}$ = 2.5–2.8‰ (calculated excluding outlier $\delta^{18}O_{quartz}$ analysis)[2]; $\delta D_{chlorite}$ = –70 to –50‰ (measured off figure 10 in Heinrich et al., 1995); δD_{fluid} = –60 to –40‰[3]
Br/Cl	0.0082–0.0162 (by mass)	0.0115 (by mass)
Ar	1–3 ppb ^{36}Ar; $^{40}Ar/^{36}Ar$ ~10,000–28,000; $^{40}Ar_E/Cl \sim 3$ to 8×10^{-4}	

[1]T_h = homogenization temperature; T_m = mineralization temperature
[2]Calculated from $\delta^{18}O_{qartz}$ range following Heinrich et al. (1989, 1995) after assuming a salinity correction of 1‰ and using Matsuhisa et al. (1979) $\Delta^{18}O_{quartzwater}$ fractionation calibration at 300°C
[3]Calculated following Heinrich et al. (1995) assuming $\Delta D_{chlorite} \sim \Delta D_{serpentine}$, and using the $\Delta D_{serpentine}$ calibration of Sakai and Tsutsumi (1978) assuming temperature = 300°C

Table 3. Alternative Metal and Fluid Sources

Metal source; fluid source	Pros	Cons
Magmatic-hydrothermal; magmatic hydrothermal	Regionally, the Williams-Naraku Magmatic Suite overlaps in age with the Mount Isa copper deposits and IOCG deposits in the Eastern subprovince Ore fluids are moderately saline, consistent with a magmatic-hydrothermal fluid	The Williams-Naraku Suite is largely developed in the eastern part of the province and not known to be present in the vicinity of Mount Isa; copper isotope data from Mount Isa differ from the signatures of magmatic-hydrothermal deposits such as porphyry copper deposits O-H isotope data from regional chlorite (± albite ± rutile) alteration zones and ore fluids do not overlap magmatic water box Br/Cl of ore and regional fluids too high for a magmatic-hydrothermal origin
Leached basalt; magmatic-hydrothermal	Regionally, the Williams-Naraku Magmatic Suite overlaps in age with the Mount Isa copper deposits and IOCG deposits in the Eastern subprovince Ore fluids are moderately saline, consistent with a magmatic-hydrothermal fluid	The Williams-Naraku Suite is largely developed in the eastern part of the province, and not known to be present in the vicinity of Mount Isa O-H isotope data from regional chlorite (± albite ± rutile) alteration zones and ore fluids do not overlap magmatic water box Br/Cl of ore and regional fluids too high for a magmatic-hydrothermal origin
Leached basalt; metamorphic	Geochemical, isotopic, and geochronological data suggest extensive leaching of basalt coeval with regional chlorite (± albite ± rutile) alteration and Mount Isa copper ore formation Alteration mineralogy of regional alteration assemblage and ore-related alteration consistent with low greenschist facies metamorphism	Timing of mineralization (D_3) postdates main contractional deformation event (D_2) (Perkins, 1984) Age of mineralization (ca. 1523 Ma) postdates main stage of Isan contractional deformation and peak metamorphism (1600–1580 Ma: Giles et al., 2006; Li et al., 2020) O-H isotope composition of ore and alteration fluids only slightly overlaps field of metamorphic fluids; ore and alteration fluids relatively saline for metamorphic fluids
Leached basalt; basinal brine	Geochemical, isotopic, and geochronological data suggest extensive leaching of basalt coeval with regional chlorite (± albite ± rutile) alteration and Mount Isa copper ore formation O-H isotope, salinity, and Br/Cl data most consistent with evolved bittern brine	Timing of brine formation and circulation problematic; the Isan orogeny, including contractional deformation and greenschist facies metamorphism, comes between brine formation and mineralization if the brines were sourced from the 1640–1590 Ma Isa superbasin The Roper superbasin may have been too young to source ca.1525 Ma brines

Abbreviation: IOCG = iron oxide copper-gold

(cf. Perkins et al., 1999), the best estimate for the age of the chlorite ± albite assemblage is ca. 1535 Ma. In contrast, Hannan et al. (1993) interpreted the epidosite as a consequence of subseafloor alteration as seen, for example, in mid-oceanic ridge basalts (Mottl, 1983) and in some volcanic-hosted massive sulfide systems (e.g., Galley, 1993). Alternatively, this alteration may have formed during regional greenschist-facies metamorphism (Hannan et al., 1993; Heinrich et al., 1995). This model suggests that the epidote + sphene assemblage was initiated as the 1790 to 1760 Ma mafic rocks were emplaced and continued during regional metamorphism, whereas the chlorite ± albite assemblage accompanied or postdated the Isan orogeny. Cooke et al. (1998) inferred that the K-feldspar + chlorite regional alteration assemblage accompanied shale-hosted Zn-Pb-Ag sulfide mineralization, a process that may have occurred multiple times between 1675 Ma (Cannington deposit) and 1575 Ma (Century deposit). The age of the sericite-dominated assemblage is unconstrained.

The high-temperature (300°–350°C) chlorite ± albite assemblage has, at ca. 1535 Ma, a similar age to that inferred for regional albitite-hosted uranium deposits and the Mount Isa copper deposit. This assemblage, together with the undated epidote + sphene and sericite assemblages, appears to exist only in the 1790 to 1760 Ma mafic rocks and not in the younger 1730 to 1660 Ma mafic rocks. In contrast, the low-temperature (<150° C; Cooke et al., 1998) K-feldspar ± chlorite assemblage, which is interpreted to be associated with the 1675 to 1575 Ma shale-hosted zinc-lead-silver mineralization, appears only present in the 1730 to 1660 Ma mafic rocks.

This alteration dichotomy is surprising as both the older and younger suites of mafic rocks were present within the basin at the time of both mineralizing events. The older mafic rocks form part of the base of the Greater McArthur basin stratigraphy and are concentrated in the Leichhardt River Domain, where a stratigraphic thickness of up to 8 km of basalt is present. At the time of shale-hosted zinc-lead-silver mineralization, these rocks were overlain by strata in the upper part of the Leichhardt superbasin and much of the overlying Calvert superbasin and were probably too deep to be affected by low-temperature, K-feldspar ± chlorite alteration associated with circulating basinal brines that strongly altered the younger rocks. Alternatively, in the older rocks, the K-feldspar ± chlorite alteration assemblage was totally overprinted by the chlorite ± albite, epidote + sphene, and sericite assemblages. All the regional alteration assemblages, except for epidote + sphene, appear to have lost copper, particularly near end member compositions, suggesting that both the 1675 to 1575 Ma and the 1540 to 1500 Ma events potentially produced copper mineralization.

The regional-scale depletion of copper from the 1790 to 1760 Ma basaltic rocks reported herein (Fig. 1B), and by Gregory (2006), supports the hypothesis of Heinrich et al. (1995) that the basalt units structurally below the Mount Isa copper deposit were the source of the contained copper. In detail, however, the pattern is complex, with several local zones of copper enrichment present near the deposit. These complexities may indicate that local structures have channelized some of the fluids and caused local copper enrichment. Geochemically, copper loss from the Eastern Creek

Volcanics is associated with chloritic alteration assemblages in the 1790 to 1760 Ma basalts (Figs. 2B, 4B) that are extensively developed regionally in the southern part of the Leichhardt River Domain. ^{40}Ar-^{39}Ar plateau ages of biotite suggest that this chloritic alteration (1534 ± 8 Ma)—where uncertainties cited herein are 2σ values as opposed to the 1σ values cited by Perkins et al. (1999)—overlaps in age with the Mount Isa copper deposit (1523 ± 6 Ma) (Perkins et al., 1999).

Spatially, the copper depletion anomaly coincides with a ^{56}Fe enrichment anomaly. Moreover, a ^{65}Cu enrichment anomaly coincides with the northern extension of the copper depletion and ^{56}Fe enrichment anomalies, just to the east of the Mount Isa copper deposit. Together with the geochronological data, the patterns of these anomalies suggest that the copper depletion and ^{56}Fe and ^{65}Cu enrichments developed as part of the mineral system that formed the Mount Isa copper deposit at ca. 1525 Ma. If true, the area of copper depletion associated with the mineral system that formed the Mount Isa copper deposit had a dimension of at least 25 × 50 km based on the ^{65}Cu anomaly.

Owing to the complex metallogeny of the Greater McArthur basin, it is likely that parts of this basin have been affected by multiple mineralizing/alteration events, raising the probability of overprinting processes. The overprinting of different alteration events, possibly ranging in age from 1790 to 1530 Ma (or younger), may account for some of the complex geochemical (Fig. 1B) and isotopic (Fig. 1C) trends observed in the data sets.

Leaching of copper from basalt

To better understand processes that produce copper-depleted and ^{65}Cu-enriched basalt, we have undertaken isotopic modeling of copper extraction assuming Rayleigh-type copper isotope fractionation during leaching. Before describing this modeling, it is important to understand the deportment of copper within unaltered basalt.

In unaltered, devitrified basalt copper will predominantly be held in three phases: (1) ferro-magnesian silicate minerals such as pyroxene and amphibole, (2) magnetite, and (3) monosulfide solid solution (MSS) (Desborough et al., 1968). In most ferro-magnesian minerals, Cu^{2+} substitutes for Fe^{2+} and/or Mg^{2+} (Ding et al., 2016; Wang et al., 2019). Similarly, as cuprospinel ($Cu^{2+}Fe_2^{3+}O_4$) is isostructural with magnetite, Cu^{2+} substitutes for Fe^{2+} (Nadoll et al., 2014; Gezzaz et al., 2023) in magnetite. Copper and other metals also occur as divalent ions in MSS.

As most reduced to slightly oxidized hydrothermal fluids carry copper in the monovalent state (e.g., Cu^+ in $CuCl_{(aq)}$), the leaching of copper from a basalt involves the reduction of copper according to reactions such as the following:

$$2CuO_{en} + 2Cl^- + 2H^+ = 2CuCl + H_2O, \quad (1)$$

$$2CuO_{mt} + 2Cl^- + 2H^+ = 2CuCl + H_2O, \quad (2)$$

and

$$4CuS_{MSS} + 7O_2 + 4Cl^- + 2H_2O = 4CuCl + 4HSO_4^-, \quad (3)$$

where the subscripts en, mt, and MSS refer to enstatite, magnetite, and monosulfide solid solution, respectively. All of these reactions involve the reduction of copper, from Cu^{2+} in the rock/mineral to Cu^+ in the ore fluid. Importantly, this process occurs even if the rock as a whole is oxidized.

As reduction fractionates light isotopes relative to heavy isotopes (e.g., Ohmoto, 1972), reactions (1) to (3) should fractionate light copper into the fluid, with isotopically heavy copper residue retained in the rock. This process will result in the ore fluids and resulting mineralization depleted in ^{65}Cu and the residual copper in the altered and leached basalt enriched in ^{65}Cu. Figure 5 shows the effect of open system behavior for reaction (1) where the isotopic composition of the residuum (leached basalt) is calculated using Rayleigh-type fractionation. These calculations done using $\Delta^{65}Cu_{CuCl\,(aq)\,-\,enstatite}$ data derived from Seo et al. (2007) and Liu et al. (2021), assuming an initial basalt $\delta^{65}Cu$ value of 0.2‰ and an alteration temperature of 300°C. For a leaching efficiency of 50 to 90% (F = 0.5–0.9 and 50–90 ppm copper loss, assuming an initial basalt concentration of 100 ppm), the Rayleigh fractionation calculations indicate that the residuum should have $\delta^{65}Cu$ of 1.0 to 2.7‰, consistent with the observed values in ^{65}Cu-enriched and copper-depleted basalt (1.0–2.4‰). This mechanism produces a leachate (i.e., ore fluid) with a $\delta^{65}Cu$ value of –0.6 to 0.2‰. We discuss isotopic variations expected from chalcopyrite deposition from such a fluid below.

Collectively, the data suggest that leached basalt is the most likely source of copper in the Mount Isa deposit. Although we cannot exclude a direct magmatic-hydrothermal metal source, this is considered unlikely given the size of the leached zone and the lack of nearby intrusive rocks. Assuming a 50% leaching efficiency of a precursor basalt containing 100 ppm copper and an areal extent of 25 × 50 km, a stratigraphic thickness of 600 m (750 km^3) for the basalt would be sufficient to provide all the copper present in the Mount Isa copper deposit. This estimate is much less than the 5- to 8-km thickness (10,000 km^3) thought to characterize much of the Leichhardt River Domain (Gibson et al., 2018). The leached volume accounts for 7.5% of the total volume of basalt, more than making up for potential inefficiencies in the leaching of copper at the source and copper precipitation at the depositional site.

Fluid source

Whereas our data strongly support leached basalt as the source of copper in the Mount Isa copper mineral system, sources of the fluids that altered the basalt are still unresolved and can include a magmatic fluid, a metamorphic fluid, or a basinal brine. Although not directly resolving this issue, these data, together with other, preexisting data, can provide some solid constraints (Table 3) and new insights into metallogenic processes.

Figure 6 compares $\delta^{65}Cu$ populations of the basaltic samples with those of ore samples from the Mount Isa copper deposit, IOCG deposits in the eastern Mount Isa province, the Candelaria (Chile) IOCG deposit, and global porphyry copper deposits. Compared with global porphyry deposits, which are accepted as having a magmatic-hydrothermal origin for both the fluids and metals, the Mount Isa ore values have a slightly lower median $\delta^{65}Cu$ and a much narrower range of values. These differences are inconsistent with a magmatic-hydrothermal origin for both the copper and ore fluids, as discussed below. This inference is supported by the O-H isotope characteristics of the Mount Isa ore and regional fluids, both

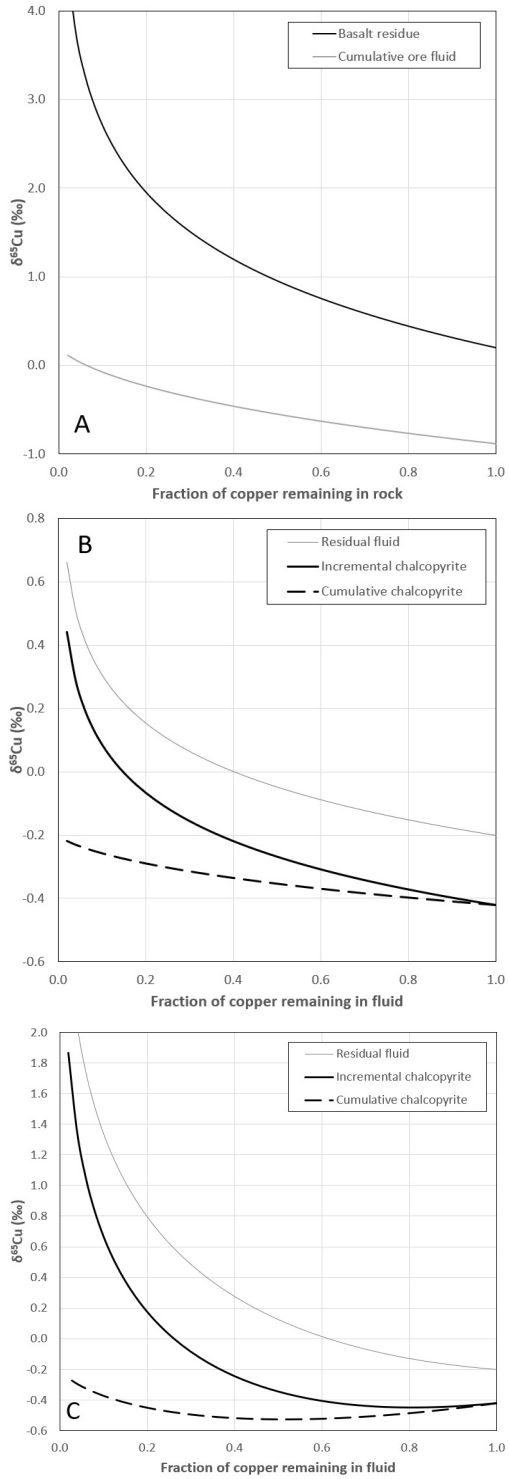

Fig. 5. Rayleigh fractionation modeling to account for (A) residual $\delta^{65}Cu$ signature of leached (residual) mafic rocks, (B) spatial variations in $\delta^{65}Cu$ in the Mount Isa copper deposit, and (C) variations in $\delta^{65}Cu$ from porphyry copper deposits. Part (A) is calculated at 300°C assuming isotopic fractionation between copper in basalt, using copper in enstatite (Liu et al., 2021) as an approximation, and aqueous CuCl (Seo et al., 2007) and an initial basalt $\delta^{65}Cu$ value of 0.2‰. Part (B) is calculated at 350°C using the experimental $\Delta^{65}Cu_{chalopyrite - Cu\ (aq)}$ value of Syverson et al. (2021). Part (C) is calculated starting from 350°C and assuming the temperature decreases as copper is precipitated. The temperature decrease has been modeled by increasing $\Delta^{65}Cu_{chalopyrite - Cu\ (aq)}$ from 0.22‰ at 350°C to 0.71‰.

of which have $\delta^{18}O$ values too low to be primary magmatic water (Fig. 5).

Figure 7 indicates that both the ore and regional fluids are most compatible with either metamorphic fluids or basinal brines. These fluids just overlap the field of metamorphic waters (Fig. 7), but the timing of mineralization postdates D_2 contraction and high-grade metamorphism associated with the Isan orogeny. This relative timing is consistent with both structural relationships at the deposit scale (Perkins, 1984) and absolute geochronological ages (Perkins et al., 1999). The timing of fluid flow after peak metamorphism thus makes a metamorphic origin less likely as an earlier phase of metamorphism would have devolatilized the rock package. Hence, even though the isotopic and other data permit a metamorphic origin for the fluids, the absolute and relative timing of peak metamorphism (1600–1580 Ma), regional alteration (ca. 1534 Ma), and mineralization (ca. 1523 Ma) make a metamorphic fluid source unlikely. Moreover, the alteration and leaching patterns are inconsistent with Barrovian-style metamorphism, as the metal leaching is localized rather than regional in scope, and because synmineralization (ca. 1535–1520 Ma) granitic intrusions are unknown in the vicinity of Mount Isa, although they occur ~100 km to the east.

The oxygen and hydrogen isotope characteristics of the ore and regional fluids are most consistent with derivation from an evolved basinal brine: the composition of the Isan fluids is bracketed by values for evolved basinal brines from the Alberta and Michigan basins (Fig. 7). A basinal brine fluid source, however, also has timing problems. The contractional phase of the Isan orogeny (1600–1580 Ma) occurred between brine formation and mineralization if the brine was sourced from the Isa superbasin. Further, the Roper superbasin, the base of which has an oldest age of ca. 1492 Ma, may be too young to have produced the mineralizing brines, even though geochronological constraints permit this possibility.

The intensity of Isan deformation broadly decreases from north to south, with the southern Leichhardt River Domain and regions to the east being the most deformed. Well to the north (e.g., Lawn Hill platform), rocks of the Isa superbasin are largely unmetamorphosed and undeformed and may have retained basinal brines. It may be that external basinal brines, derived either from the less-deformed parts of the Calvert or Isa superbasins or from the Roper superbasin, flooded into the Leichhardt River Domain during postorogenic collapse, after the main contractional phase of the Isan orogeny (e.g., Li et al., 2020). In any case, our and previous data do not allow unequivocal identification of the source of the Mount Isa copper ore fluids but do strongly suggest a basinal brine source.

Ore deposition

Sanislav et al. (2023) demonstrated that copper isotope values are zoned in the Mount Isa copper deposit relative to major structures, with $\delta^{65}Cu$ increasing from –0.7 to 0.0‰ within 50 m of, to 0.0 to 0.9‰ 200 m or more from, such structures. Assuming that the fluids moved outward from these structures, this spatial distribution can be explained by Rayleigh fractionation during ore deposition (Fig. 5B). At 350°C, chalcopyrite precipitated adjacent to the feeder structures will have a $\delta^{65}Cu$ value ~0.2‰ lower than that of the entering ore fluid. 350°C was used for this modeling as there are experimental data for

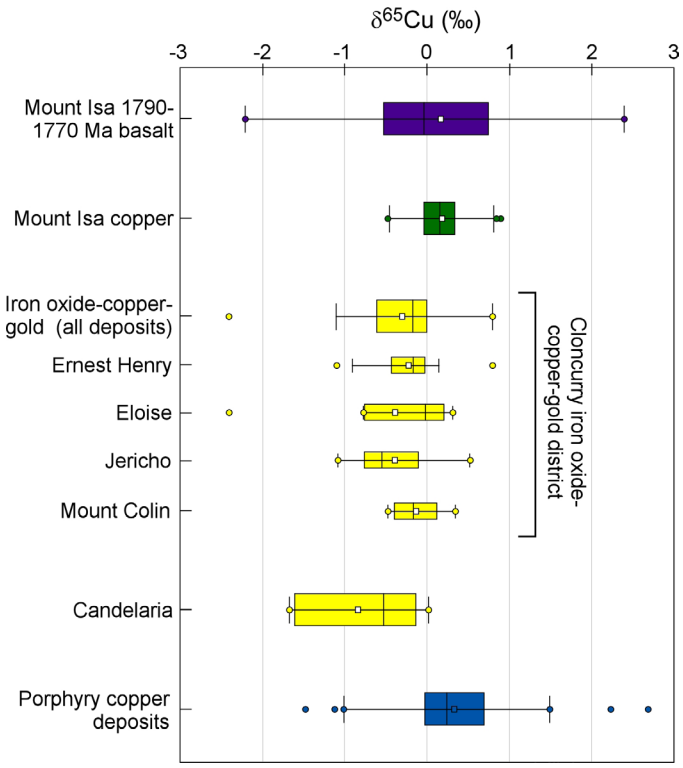

Fig. 6. Box-and-whisker diagram comparing δ^{65}Cu data from the Mount Isa regional 1790 to 1760 Ma basaltic rocks (n = 26) with the Mount Isa copper deposit (n = 104; Sanislav et al., 2023), iron oxide copper-gold deposits from the eastern Mount Isa province (Combined, n = 43; Jericho, n = 16; Ernest Henry, n = 13; Elouise, n = 9; Mount Colin, n = 5; Appendix 2), the Candelaria (Chile) iron oxide copper-gold deposit (n = 9; Appendix 2) and global porphyry copper deposits (n = 188; Maher et al., 2003; 2005; Graham et al., 2004; Mathur et al., 2005, 2009, 2010, 2012, 2013, 2014; Li et al., 2010; Mirnejad et al., 2010; Palacios et al., 2011; Braxton and Mathur, 2014; Asadi et al., 2015; Duan et al., 2016; Gregory and Mathur, 2017; Wu et al., 2017; Kim et al., 2019; Chiaradia et al., 2023). Boxes indicate the 75th and 25th percentiles, with median shown by line in the center of the box. Whiskers indicate the 5th and 95th percentiles. Average is indicated by open square in the box center. Outliers and/or maxima/minima indicated by solid circles.

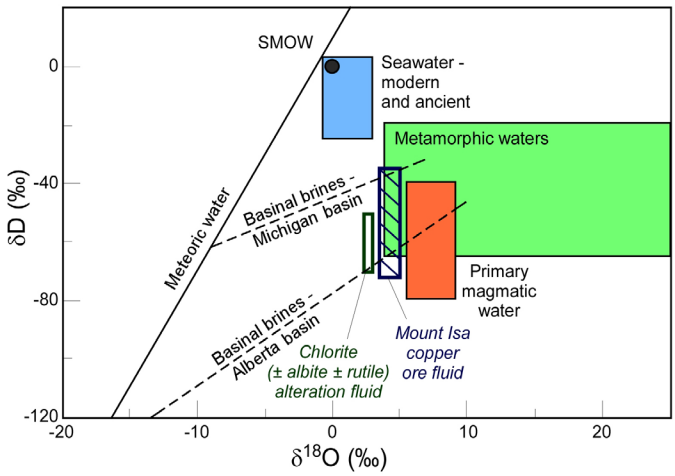

Fig. 7. δ^{18}O versus δD diagram showing isotopic composition of Mount Isa copper ore fluids and regional chloritic alteration fluids in comparison with values for seawater, meteoric fluids, metamorphic fluids, magmatic fluids, and evolved basinal brines (modified after Heinrich et al., 1989). Abbreviation: SMOW = standard mean ocean water.

$\Delta^{65}Cu_{chalopyrite-Cu(aq)}$ (Syerson et al., 2021). Moreover, the fractionation factor for chalcopyrite deposition should increase slightly at the lower temperature (e.g., 300°C) of ore formation, although not affecting the general trend shown. Using the midpoint of the modeled range of fluid δ^{65}Cu leached from basalt (–0.2‰), initially precipitated chalcopyrite will have δ^{65}Cu ~ –0.4‰. The precipitation of ^{65}Cu-poor chalcopyrite relative to the ore fluid will, via Rayleigh fractionation, enrich the residual fluid in ^{65}Cu, leading to the precipitation of progressively ^{65}Cu-enriched chalcopyrite and an increase in δ^{65}Cu away from major structures. The modeled variation in δ^{65}Cu, from an initial value –0.4‰ to 0.1 to 0.5‰ when the fluid has lost 90% or more of its copper (Fig. 5B), matches well the observed distribution in the region.

Some ^{65}Cu-enriched samples are also enriched in copper, with values of up to 1,220 ppm Cu. According to the modeling above, highly ^{65}Cu-enriched sulfide mineralization can be produced in the distal parts of a depositional site. Although the values reported for the Mount Isa copper deposit do not reach the δ^{65}Cu values observed in these Cu-rich samples, it is possible that the Cu-rich, high-δ^{65}Cu samples represent very distal manifestation of mineralized zones.

As discussed earlier and shown in Figure 6, the δ^{65}Cu characteristics of porphyry copper ores have a much larger, although overlapping range, with those for Mount Isa. For Mount Isa, the observed δ^{65}Cu range in copper ores can be explained by Rayleigh fractionation as the ore fluids pass through the mineralized zone. A similar mechanism may also account for the observed variations in porphyry copper ores, particularly if temperature decreases during mineralization are considered. One mechanism contributing to porphyry copper ore deposition is thought to be temperature decrease (e.g., Beane and Titley, 1981), as expected if magmas exsolved high-temperature magmatic-hydrothermal fluids into a low-temperature, upper crustal environment.

Figure 5C models such a system, whereby $\Delta^{65}Cu_{chalcopyrite-Cu(aq)}$ increases as temperature decreases. This modeling suggests that the combination of Rayleigh fractionation and decreasing temperature can account for variations in δ^{65}Cu values in magmatic-hydrothermal systems by involving a significant drop in temperature during mineralization. For porphyry copper deposits, the presence and potential transport in a vapor phase may also increase the variability in δ^{65}Cu. The lighter δ^{65}Cu signature of IOCG ores from the eastern Mount Isa province (Cloncurry district) and Candelaria (Chile) suggests differences in either the copper source or the mechanism of ore deposition, or both. The restricted range in δ^{65}Cu for the Mount Isa mineral system, compared to porphyry copper deposits, may suggest that temperature decrease was not as important as in porphyry copper systems.

Decoupling of copper and iron isotope fractionation during regional alteration

As described above, δ^{65}Cu and δ^{56}Fe values are not correlated, suggesting that isotopic fractionation of these elements during regional alteration was decoupled. In the samples

analyzed for $\delta^{65}Cu$ and $\delta^{56}Fe$, the relative range in copper concentrations (5–300 ppm; Cu_{max}/Cu_{min} = 60; excluding one outlier at 1,220 ppm) is much larger than the range in iron concentrations (6.94–16.90% total Fe_2O_3; Fe_{max}/Fe_{min} = 2.4; excluding one outlier with 36.75% total Fe_2O_3). This pattern indicates that copper was highly mobile, whereas iron was relatively immobile during alteration of the mafic rocks. Moreover, in absolute terms, the amount of metal mobilized to cause a major shift in iron concentrations is much greater than that required for a major shift in copper concentrations. The interpretation that iron in this context is immobile is substantiated by Heinrich et al. (1995), who found that total iron plotted on the isocon defined by immobile elements such as zirconium, titanium, and aluminum. In contrast, FeO plotted below the isocon (i.e., was lost), whereas Fe_2O_3 plotted above the isocon (i.e., was gained).

The main effect of alteration on iron in regional mafic rocks was, in most cases, oxidation (i.e., conversion of Fe^{2+} to Fe^{3+}) and not mobility. The limited mobility of iron during alteration in this type of system restricted the fractionation of ^{56}Fe because, relatively, not much iron was added or lost, causing a restricted range in $\delta^{56}Fe$ values. In contrast, the loss of copper to a hydrothermal fluid, as discussed above, caused significant fractionation of ^{65}Cu, leading to large variability in $\delta^{65}Cu$ values. Hence, the decoupling of $\delta^{65}Cu$ and $\delta^{56}Fe$ may be simply due to different geochemical behavior during alteration: copper was highly mobile, coupled with strong isotopic fractionation, whereas iron was relatively immobile with weak fractionation. The decoupling may also be due to the greater variety of mineralogical and/or petrological sitings of iron relative to copper.

Metallogenic and exploration implications

Our results indicate that the Mount Isa copper deposit is located along the western margin of a ^{65}Cu-enriched zone with dimensions of 25 × 50 km. We interpret this zone to represent the minimum extent of the Mount Isa copper mineral system and an indication of the size of a leached zone that served as the copper source for a large, world-class deposit. Although not documented using copper isotopes, similar large-scale copper leaching has been noted in the Humboldt Mafic Complex in Nevada (Johnson and Barton, 2000) and in the Panorama volcanic-hosted massive system in Western Australia (Brauhart et al., 2001). The Mount Isa system is located along the western margin of the Leichhardt River Domain and does not appear to extend outside of this zone, suggesting that the mineral system was confined by preexisting architecture. No other $\delta^{65}Cu$ anomalies of similar scale are observed in our data set, possibly indicating that the Mount Isa copper mineral system is unique in the Mount Isa province. Our study also indicates that $\delta^{65}Cu$ can be used to identify zones of copper depletion using a relatively small number of samples over a large area and suggests that copper isotopes may be useful at the regional scale to identify the footprint of mineral systems.

Figure 6 shows that the ranges of copper isotope fractionation from IOCG deposits are comparable to each other but smaller than reported for porphyry copper deposits. Magmatic processes, including thermal gradients, operating during porphyry copper deposition, expand total ranges in $\delta^{65}Cu$ values and suggest that the IOCG clan of deposits is isotopically different from porphyry copper deposits. The lower copper isotope mean values for the system could be representing copper reduction by Cl-rich brine fluids for these systems. Presently, the metallic isotope data set does not extend to the east into the Cloncurry IOCG district, but there is evidence of copper depletion along the eastern margin of the region for which coverage does exist. It will prove valuable to see the $\delta^{65}Cu$ and $\delta^{56}Fe$ data when the present survey is extended to the east to cover the Cloncurry IOCG district.

Conclusions

Our study of regional variations in $\delta^{65}Cu$ values for regional mafic rocks in the Mount Isa province supports existing studies that indicate that the copper source was these rocks. The mafic copper isotope data define a 25 × 50 km ^{65}Cu-enriched zone to the east of the Mount Isa copper deposit within the Leichhardt River Domain. We interpret this zone, which overlaps the northern part of a Cu- and ^{56}Fe-depleted zone to the south, as the most likely source of copper and an indication of the minimum size of the mineral system that produced the Mount Isa copper deposit. Raleigh modeling suggests that the leaching of basalt would produce the observed ^{65}Cu-enriched zone and a fluid $\delta^{65}Cu$ value of around –0.2‰.

The copper and iron isotope values, when combined with other isotopic and geochemical data, strongly suggest that the ore fluid for the Mount Isa copper deposit was an evolved basinal brine, and not a metamorphic or magmatic-hydrothermal fluid, although neither of these latter possibilities can be totally excluded. The source of the basinal brine cannot be confidently established: possibilities include either brines derived from the undeformed part of the Isa or Calvert superbasins to the north, or brines from the overlying Roper superbasin.

Comparison of the Mount Isa ore $\delta^{65}Cu$ data (Sanislav et al., 2023) suggests significant differences in isotopic characteristics between this deposit, porphyry copper deposits, and IOCG deposits. Simple, isothermal Rayleigh fractionation from an entering ore fluid with $\delta^{65}Cu \sim -0.2$‰ can account for the isotopic zonation relative to major structures documented by Sanislav et al. (2023). The large range in $\delta^{65}Cu$ observed in porphyry copper deposits can be explained by Rayleigh fractionation down a thermal gradient as would be expected when high-temperature magmatic-hydrothermal fluids are introduced into a relatively cool, upper crustal environment. The lower mean $\delta^{65}Cu$ value in the Cloncurry IOCG deposits may be indicative of a lower initial $\delta^{65}Cu$ value of the entering fluids. More detailed analysis of regional $\delta^{65}Cu$ and ore $\delta^{65}Cu$ variations in this region is the subject of ongoing research.

Acknowledgments

This contribution benefited from reviews by Nick Oliver, Yanbo Cheng, Evgeniy Bastrakov, and two anonymous reviewers. The first anonymous reviewer is particularly thanked for suggesting the use of ternary diagrams for discussing geochemical and isotopic trends. Associate Editor John Slack is also thanked for providing insightful guidance for revisions and making sure we minded our p's and q's, or in this case the z's and s's. RM and AS acknowledge support from U.S. National Science Foundation EAR grants 2233426, 2419986, 2233425,

and 2214119. This contribution is published with permission of the chief executive officer of Geoscience Australia.

REFERENCES

Abbott, S.T., Sweet, I.P., Plumb, K.A., et al., 2001, Roper region: Urapunga and Roper River special, Northern Territory, 2nd ed.: Northern Territory Geological Survey, geological map series explanatory notes, Sheets SD53-10, SD53-11, scale 1:250,000, https://geoscience.nt.gov.au/gemis/ntgsjspui/handle/1/81859.

Abu Sharib, A.S.A.A., and Sanislav, I.V., 2013, Polymetamorphism accompanied switching in horizontal shortening during Isan orogeny: Example from the Eastern fold belt, Mount Isa inlier, Australia: Tectonophysics, v. 587, p. 146–167.

Anderson, J., Carson, C., Lewis, C., et al., 2019, Exploring for the future: New U-Pb geochronology for the South Nicholson region and implications for stratigraphic correlations: ASEG Extended Abstracts, v. 2019:1, p. 1–5, https://doi.org/10.1080/22020586.2019.12073005.

Asadi, S., Mathur, R., Moore, F., and Zarasvandi, A., 2015, Copper isotope fractionation in the Meiduk porphyry copper deposit, northwest of Kerman Cenozoic magmatic arc, Iran: Terra Nova, v. 27, p. 36–41.

Beane, R.E., and Titley, S.R., 1981, Porphyry copper deposits: Part II. Hydrothermal alteration and mineralization: Economic Geology 75th Anniversary Volume, p. 235–269.

Betts, P.G., Giles, D., Mark, G., Lister, G.S., Goleby, B.R., and Aillères, L., 2006, Synthesis of the Proterozoic evolution of the Mt Isa inlier: Australian Journal of Earth Sciences, v. 53, p. 187–211.

Bodorkos, S., Crowley, J.L., Claoué-Long, J.C., Anderson, J.R., and Magee, Jr., C.W., 2021, Precise U-Pb baddeleyite dating of the Derim Derim dolerite, McArthur basin, Northern Territory: Old and new SHRIMP and ID-TIMS constraints: Australian Journal of Earth Sciences, v. 68, p. 36–50.

Brauhart, W.W., Huston, D.L., Groves, D.I., Mikucki, E.J., and Gardoll, S.J., 2001, Geochemical mass-transfer patterns as indicators of the architecture of a complete volcanic-hosted massive sulfide hydrothermal alteration system, Panorama district, Pilbara, Western Australia: Economic Geology, v. 96, p. 1263–1278.

Braxton, D.P., and Mathur R., 2014, Copper isotopic vectors to supergene enrichment: Leaches cap isotopic footprint of the Quellaveco porphyry copper deposit, southern Peru: Society of Economic Geologists, SEG 2014: Building Exploration Capability for the 21st Century, Denver, Colorado, 2014, Proceedings.

Cave, B., Lilly, R., and Barovich, K., 2020, Textural and geochemical analysis of chalcopyrite, galena and sphalerite across the Mount Isa Cu to Pb-Zn transition: Implications for a zoned Cu-Pb-Zn system: Ore Geology Reviews, v. 124, article 103647, https://doi.org/10.1016/j.oregeorev.2020.103647.

Champion, D.C., and Huston, D., 2023, Application of neodymium isotopies to ore deposits and metallogenic terranes; Using regional isotopic maps and the mineral systems concept, *in* Huston, D.L., and Gutzmer, J., eds., Isotopes in economic geology, metallogenesis and exploration: Cham, Switzerland, Springer, p. 123–154.

Champion, D.C., Huston, D.L., Bastrakov, E., et al., 2020a, Alteration of mafic igneous rocks of the southern McArthur basin: Comparisons with the Mount Isa region and implications for basin-hosted base metal deposits: Exploring for the future: Extended abstracts, Geoscience Australia, Canberra, https://doi.org/10.11636/134206.

Champion, D.C., Huston, D.L., Cross, A., Jarrett, A., Bastrakov, E., and Thorne, J., 2020b, Geochemistry and age of the greater McArthur basin: Base line geochemical studies and implications for basin-hosted mineral systems: Annual Geoscience Exploration Seminar (AGES), Alice Springs, Northern Territory, March 24–25, 2020, Proceedings, p. 105–116.

Champion, D.C., Huston, D., Main, P., et al., 2020c, Exploring for the future baseline whole rock geochemistry of northern Australia: Data release—geochemistry of drill core samples from the McArthur basin, Lawn Hill platform and Tomkinson province, Northern Territory and Queensland: Geoscience Australia Record 2020/41, https://doi.org/10.11636/Record.2020.041.

Chiaradia, M., Mathur, R., Vennemann, T., and Simon, A., 2023, Applications of radiogenic and transition metal isotopes to the study of metallic mineral deposits: Elsevier, Amsterdam, Netherlands, Reference Module in Earth Systems and Environmental Sciences, https://doi.org/10.1016/B978-0-323-99762-1.00010-3.

Cooke, D.R., Bull, S.W., Donovan, S., and Rogers, J.R., 1998, K-metasomatism and base metal depletion in volcanic rocks from the McArthur basin, Northern Territory: Implications for base metal mineralization: Economic Geology, v. 93, p. 1237–1263.

Cox, K., Bell, J., and Pankhurst, R., 1979, The interpretation of igneous rocks: London, George Allen and Unwin, 450 p.

Desborough, G.A., Anderson, A.T., and Wright, T.L., 1968, Mineralogy of sulfides from certain Hawaiian basalts: Economic Geology, v. 63, p. 636–644.

Ding, L., Darie, C., Colin, C.V., and Bordet, P., 2016, $Cu_{0.8}Mg_{1.2}Si_2O_6$: A copper-bearing silicate with the low-clinopyroxene structure: Mineralogical Magazine, v. 80, p. 325–335.

Duan, J., Tang, J., Li, Y., et al., 2016, Copper isotopic signature of the Tiegelongnan high-sulfidation copper deposit, Tibet: Implications for its origin and mineral exploration: Mineralium Deposita, v. 51, p. 591–602.

Duncan, R.J., Stein, H.J., Evans, K.A., Hitzman, M.W., Nelson, E.P., and Kirwin, D.J., 2011, A new geochronological framework for mineralization and alteration in the Selwyn-Mount Dore corridor, Eastern fold belt, Mount Isa inlier, Australia: Genetic implications for iron oxide copper-gold deposits: Economic Geology, v. 106, p. 169–192.

Galley, A.G., 1993, Semi-conformable alteration zones in volcanogenic massive sulphide districts: Journal of Geochemical Exploration, v. 48, p. 175–200.

Gezzaz, H., Ciobanu, C.L., Cook, N.J., et al., 2023, Copper-bearing magnetite and delafossite in copper smelter slags: Minerals, v. 13, article 1374, https://doi.org/10.3390/13111374.

Gibson, G.M., and Edwards, S., 2020, Basin inversion and structural architecture as constraints on fluid flow and Pb-Zn mineralization in the Paleo-Mesoproterozoic sedimentary sequences of northern Australia: Solid Earth, v. 11, p. 1205–1226.

Gibson, G.M., Meixner, A.J., Withnall, I.W., et al., 2016, Basin architecture and evolution in the Mount Isa mineral province, northern Australia: Constraints from deep seismic reflection profiling and implications for ore genesis: Ore Geology Reviews, v. 76, p. 414–441.

Gibson, G.M., Champion, D.C., Withnall, I.W., Neumann, N.L., and Hutton, L.J., 2018, Basaltic magmatism in the 1800–640 Ma Leichhardt and Calvert superbasins of northern Australia: A cautionary note on the use of large igneous provinces (LIPs) as temporal markers of continental breakup: Large Igneous Provinces Commission, August 2018 LIP of the Month, https://www.largeigneousprovinces.org/18aug.

Giles, D., Betts, P.G., Ailléres, L., Hulscher, B., Hough, M., and Lister, G.S., 2006, Evolution of the Isan orogeny at the southeastern margin of the Mt Isa inlier: Australian Journal of Earth Sciences, v. 53, p. 91–108.

Graham, S., Pearson, N., Jackson, S., Griffin, W., and O'Reilly, S.Y., 2004, Tracing Cu and Fe from source to porphyry: In situ determination of Cu and Fe isotope ratios in sulfides from the Grasberg Cu-Au deposit: Chemical Geology, v. 207, p. 147–169.

Gregory, M.J., 2006, Copper mobility in the Eastern Creek Volcanics, Mount Isa, Australia: Evidence from laser ablation ICP-MS of iron-titanium oxides: Mineralium Deposita, v. 41, p. 691–711.

Gregory, M.J., and Mathur, R., 2017, Understanding copper isotope behavior in the high temperature magmatic-hydrothermal porphyry environment: Geochemistry, Geophysics, Geosystems, v. 18, p. 4000-4015.

Gregory, M.J., Wilde, A.R., and Jones, P.A., 2005, Uranium deposits of the Mount Isa region and their relationship to deformation, metamorphism, and copper deposition: Economic Geology, v. 100, p. 537–546.

Halley, S.W., 2020, Mapping magmatic and hydrothermal processes from routine exploration geochemical analyses: Economic Geology, v. 115, p. 489–503, https://doi.org/10.5382/econgeo.4722.

Halley, S.W., Wood, D., Stoltze, A., Godfroid, J., Goswell, H., and Jack, D., 2016, Using multielement geochemistry to map multiple components of a mineral system: Case study from a sediment-hosted Cu-Ni camp, NW Province, Zambia: SEG Newsletter, v. 104, p. 1, 15–21.

Hannan, K.W., Golding, S.D., Herbert, H.K., and Krouse, H.R., 1993, Contrasting alteration assemblages in metabasites from Mount Isa, Queensland: Implications for copper ore genesis: Economic Geology, v. 88, p. 1135–1175.

Heinrich, C.A., Andrew, A.S., Wilkins, R.W.T., and Patterson, D.J., 1989, A fluid inclusion and stable isotope study of synmetamorphic copper ore formation at Mount Isa, Australia: Economic Geology, v. 84, p. 529–550.

Heinrich, C.A., Bain, J.H.C., Fardy, J.J., and Waring, C.L., 1993, Br/CI geochemistry of hydrothermal brines associated with Proterozoic metasediment-hosted copper mineralization at Mount Isa, northern Australia: Geochimica et Cosmochimica Acta, v. 57, p 2991–3000.

Heinrich, C.A., Bain, J.H.C., Mernagh, T.P., Wyborn, L.A.I., Andrew, A.S., and Waring, C.L., 1995, Fluid and mass transfer during metabasalt alteration and copper mineralization at Mount Isa, Australia: Economic Geology, v. 90, p. 705–730.

Huston, D.L., Stevens, B., Southgate, P.N., Muhling, P., and Wyborn, L., 2006, Australian Zn-Pb-Ag ore-forming systems: A review and analysis: Economic Geology, v. 101, p. 1117–1157.

Huston, D.L., Champion, D.C., Czarnota, K., et al., 2023, Zinc on the edge—isotopic and geophysical evidence that cratonic edges control world-class shale-hosted zinc-lead deposits: Mineralium Deposita, v. 58, p. 707–729, https://doi.org/10.1007/s00126-022-01153-9.

Jackson, M.J., Sweet, I.P., Page, R.W., and Bradshaw, B.E., 1999, The South Nicholson and Roper Groups: Evidence for the early Mesoproterozoic Roper superbasin: Australian Geological Survey Organisation Record, v. 1999/19, p. 36–59, http://pid.geoscience.gov.au/dataset/ga/30870.

Jackson, M.J., Scott, D.L., and Rawlings, D.J., 2000, Stratigraphic framework for the Leichhardt and Calvert superbasins: Review and correlations of the pre-1700 Ma successions between Mount Isa and McArthur River: Australian Journal of Earth Sciences, v. 47, p. 381–403.

Johnson, D.A., and Barton, M.D., 2000, Time-space development of an external brine-dominated, igneous-driven hydrothermal system: Humboldt Mafic Complex, western Nevada: Society of Economic Geologist Guidebook Series, v. 32, p. 127–143.

Kempton, P.D., Mathur, R., Harmon, R.S., Bell, A., Hoefs, J., and Shaulis, B., 2022, Cu-isotope evidence for subduction modification of lithospheric mantle: Geochemistry, Geophysics, Geosystems, v. 23, e2022GC010436.

Kendrick, M.A., Duncan, R., and Phillips, D., 2006, Noble gas and halogen constraints on mineralizing fluids of metamorphic versus surficial origin: Mt Isa, Australia: Chemical Geology, v. 235, p. 325–351.

Kim, Y., Lee, I., Oyungerel, S., Jargal, L., and Tsedenbal, T., 2019, Cu and S isotopic signatures of the Erdenetiin Ovoo porphyry Cu-Mo deposit, northern Mongolia: Implications for their origin and mineral exploration: Ore Geology Reviews, v. 104, p. 656–669.

Large, R.R., Bull, S.W., McGoldrick, P.J., Derrick, G., Carr, G., and Walters, S., 2005, Stratiform and strata-bound Zn-Pb-Ag deposits in Proterozoic sedimentary basins, northern Australia: Economic Geology 100th Anniversary Volume, p. 931–963.

Li, J., Pourteau, A., Ki, Z.X., et al., 2020, Heterogeneous exhumation of the Mount Isa orogen in NE Australia after 1.6 Ga Nuna assembly: New high-precision $^{40}Ar/^{39}Ar$ thermochronological constraints: Tectonics, v. 39, e2020TC006129, https://doi.org/10.1029/2020TC006129.

Li, W., Jackson, S.E., Pearson, N.J., and Graham, S., 2010, Copper isotopic zonation in the Northparkes porphyry Cu-Au deposit, SE Australia: Geochimica et Cosmochimica Acta, v. 74, p. 4078–4096.

Lister, G.S., O'Dea, M.G., and Somaia, I., 1999, A tale of two synclines: Rifting, inversion and transpressional popouts at Lake Julius, northwestern Mount Isa terrane, Queensland: Australian Journal of Earth Sciences, v. 46, p. 233–250.

Liu, S., Li, Y., Liu, J., Yang, Z., Liu, J., and Shi, Y., 2021, Equilibrium Cu isotope fractionation in copper minerals: A first-principles study: Chemical Geology, v. 564, p. 120060, https://doi.org/10.1016/j.chemgeo.2021.120060.

Liu, S.A., Huang, J., Liu, J., et al., 2015, Copper isotope composition of the silicate Earth: Earth and Planetary Science Letters, v. 427, p. 95–103, https://doi.org/10.1016/j.epsl.2015.06.061.

Maher, K.C., Ramos, F.C., Larson, P.B., and Anonymous, 2003, Copper isotope characteristics of the Cu (+Au, Ag) skarn at Coroccohuayco, Peru [abs.]: Geological Society of America Abstracts with Programs, v. 35, no. 6, p. 518.

Maher, K.C., Wood, S., Larson, P., and Anonymous, 2005, Causes of variations in copper isotope ratios in the porphyry/skarn ore environment: Sources or processes? [abs.]: Geological Society of America Abstracts with Programs, v. 37, no. 7, p. 315.

Mathur, R., and Zhao, Y., 2023, Copper isotopes used in mineral exploration, *in* Huston, D.L., and Gutzmer, J., eds., Isotopes in economic geology, metallogenesis and exploration: Cham, Switzerland, Springer, p. 433–450.

Mathur, R., Ruiz, J., Titley, S., Liermann, L., Buss, H., and Brantley, S.L., 2005, Cu isotopic fractionation in the supergene environment with and without bacteria: Geochimica et Cosmochimica Acta, v. 69, p. 5233–5246.

Mathur, R., Titley, S., Barra, F., et al., 2009, Exploration potential of Cu isotope fractionation in porphyry copper deposits: Journal of Geochemical Exploration, v. 102, p. 1–6.

Mathur, R., Dendas, M., Titley, S., and Phillips, A., 2010, Patterns in the copper isotope composition. of minerals in porphyry copper deposits in southwestern United States: Economic Geology, v. 105, p. 1457–1467.

Mathur, R., Ruiz, J., Casselman, M.J., Megaw, P., and van Egmond, R., 2012, Use of Cu isotopes to distinguish primary and secondary Cu mineralization in the Cañariaco Norte porphyry copper deposit, northern Peru: Mineralium Deposita, v. 47, p. 755–762.

Mathur, R., Munk, L., Nguyen, M., Gregory, M., Annell, H., and Lang, J., 2013, Modern and paleofluid pathways revealed by Cu isotope compositions in surface waters and ores of the Pebble porphyry Cu-Au-Mo deposit, Alaska: Economic Geology, v. 108, p. 529–541.

Mathur, R., Munk, L.A., Townley, B., et al., 2014, Tracing low-temperature aqueous metal migration in mineralized watersheds with Cu isotope fractionation: Applied Geochemistry, v. 51, p. 109–115.

Matsuhisa, Y., Goldsmith, J.R., and Clayton, R.N., 1979, Oxygen isotope fractionation in the system quartz-albite-anorthite-water: Geochimica et Cosmochimica Acta, v. 43, p. 1131–1140.

McGoldrick, P.J., and Keays, R.R., 1990, Mount Isa copper and lead-zinc-silver ores; coincidence or cogenesis?: Economic Geology, v. 85, p. 641–650.

Mirnejad, H., Mathur, R., Einali, M., Dendas, M., and Alirezaei, S., 2010, A comparative copper isotope study of porphyry copper deposits in Iran: Geochemistry: Exploration, Environment, Analysis, v. 10, p. 413–418, https://doi.org/10.1144/1467-7873/09-229.

Mottl, M.J., 1983, Metabasalts, axial hot springs, and the structure of hydrothermal systems at mid ocean ridges: Geological Society of America Bulletin, v. 94, p. 161–180.

Nadoll, P., Angerer, T., Mauk, J.L., French, D., and Walshe, J., 2014, The chemistry of hydrothermal magnetite: A review: Ore Geology Reviews, v. 61, p. 1–32, https://doi.org/10.1016/j.oregeorev.2013.12.013.

Ohmoto, H., 1972, Systematics of sulfur and carbon isotopes in hydrothermal ore deposits: Economic Geology, v. 67, p. 551–579.

Palacios, C., Rouxel, O., Reich, M., Cameron, E., and Leybourne, M., 2011, Pleistocene recycling of copper at a porphyry system, Atacama Desert, Chile: Cu isotope evidence: Mineralium Deposita, v. 46, p. 1–7.

Page, R.W., Jackson, M.J., and Krassay, A.A., 2000, Constraining sequence stratigraphy in north Australian basins: SHRIMP U-Pb zircon geochronology between Mt Isa and McArthur River: Australian Journal of Earth Sciences, v. 47, p. 431–459, https://doi.org/10.1046/j.1440-0952.2000.00797.x.

Perkins, W.G., 1984, Mount Isa silica dolomite and copper orebodies: The result of a syntectonic hydrothermal alteration system: Economic Geology, v. 79, p. 601–637.

Perkins, W.G., 1998, Timing of formation of Proterozoic stratiform fine-grained pyrite: Post-diagenetic cleavage replacement at Mount Isa?: Economic Geology, v. 93, p. 1153–1164.

Perkins, C., Heinrich, C.A., and Wyborn, L.A.I., 1999, $^{40}Ar/^{39}Ar$ geochronology of copper mineralization and regional alteration, Mount Isa, Australia: Economic Geology, v. 94, p. 23–36.

Polito, P.A. Kyser, T.K, and Stanley, C., 2009, The Proterozoic, albitite-hosted, Valhalla uranium deposit, Queensland, Australia: A description of the alteration assemblage associated with uranium mineralisation in diamond drill hole V39: Mineralium Deposita, v. 44, p. 11–40.

Sakai, H., and Tsutsumi, M., 1978, D/H fractionation factors between serpentine and water at 100° to 500°C and 2000 bar water pressure, and the D/H ratios of natural serpentines: Earth and Planetary Science Letters, v. 40, p. 231–242.

Sanislav, I.V., Mathur, R., Rea, P., et al., 2023, A magmatic copper and fluid source for the sediment-hosted Mount Isa deposit: Geochemical Perspectives Letters, v. 27, p. 26–31.

Seo, J.H., Lee, S.K., and Lee, I., 2007, Quantum chemical calculations of equilibrium copper (I) isotope fractionations in ore-forming fluids: Chemical Geology, v. 243, p. 225–237.

Sossi, P.A., Halverson, G.P., Nebel, O., and Eggins, S.M., 2015, Combined separation of Cu, Fe and Zn from rock matrices and improved analytical protocols for stable isotope determination: Geostandards and Geoanalytical Research, v. 39, p. 129–149.

Southgate, P.N., Bradshaw, B.E., Domagala, J., et al., 2000, Chronostratigraphic basin framework for Palaeoproterozoic rocks (1730–1575Ma) in northern Australia and implications for base-metal mineralisation: Australian Journal of Earth Sciences, v. 47, p. 461–483, https://doi.org/10.1046/j.1440-0952.2000.00787.x.

Southgate, P.N., Neumann, N.L., and Gibson, G.M., 2013, Depositional systems in the Mt Isa inlier from 1800 Ma to 1640 Ma: Implications for Zn-Pb-Ag mineralisation: Australian Journal of Earth Sciences, v. 60, p. 157–173.

Syverson, D., Borrok, D., Niebuhr, S., and Seyfried, W., 2021, Chalcopyrite-dissolved Cu isotope exchange at hydrothermal conditions: Experimental constraints at 350°C and 50 MPa: Geochimica et Cosmochimica Acta, v. 298, https://doi.org/10.1016/j.gca.2021.02.005.

Wang, G.R., Yang, H.Y., Liu, Y.Y., Tong, L.L., and Auwalu, A., 2019, The alteration mechanism of copper-bearing biotite and leachable property of

copper-bearing minerals in the Mulyashy copper mine, Zambia: Scientific Reports, v. 9, article 15050, https://doi.org/10.1038/s41598-019-50519-z.
Waring, CL., 1990, Genesis of the Mount Isa copper ore system: Ph.D. dissertation, Melbourne, Australia, Monash University, 409 p.
West, H.B., Garcia, M.O., Gerlach, D.C., and Romano, J., 1992, Geochemistry of tholeiites from Lanai, Hawaii: Contributions to Mineralogy and Petrology, v. 112, p. 520–542.
Williams, P.J., 2022, "Magnetite-group" IOCGs with special reference to Cloncurry (NW Queensland) and northern Sweden: Settings, alteration, deposit characteristics, fluid sources and their relationship to apatite-rich iron ores: Geological Association of Canada, Special Paper 52, p. 53–68.
Williams, P.J., Barton, M.D., Johnson, D.A, et al., 2005, Iron oxide copper-gold deposits: Geology, space-time distribution, and possible modes of origin: Economic Geology 100th Anniversary Volume, p. 371–404.
Withnall, I.W., and Hutton, L.J., 2013, Chapter 2: North Australian craton, *in* Jell, P.A., ed., Geology of Queensland: Brisbane, Geological Survey of Queensland, p. 23–112.
Wu, L.Y., Hu, R.Z., Li, X.F., Liu, S.A., Tang, Y.W., and Tang, Y.Y., 2017, Copper isotopic compositions of the Zijinshan high-sulfidation epithermal Cu-Au deposit, South China: Implications for deposit origin: Ore Geology Reviews, v. 83, p. 191–199.
Wyborn, L.A.I., 1987, The petrology and geochemistry of alteration assemblages in the Eastern Creek Volcanics, as a guide to copper and uranium mobility associated with regional metamorphism and deformation, Mount Isa, Queensland: Geological Society of London Special Publications, v. 33, p. 425–434.

David Huston received his PhD in 1990, then was a postdoctoral fellow at the University of Tasmania before moving to the Geological Survey of Canada in 1992. He returned to Australia in 1995 to become a research scientist at Geoscience Australia, retiring in 2025. Since retiring, Huston has continued his research through affiliations with the Australian National University, the University of Tasmania, and Monash University. His primary research interests include the geology, geochemistry, and geophysics of zinc deposits, the relationship of metallogenesis to tectonics and Earth evolution, and the economics of resource development.